Computational Analysis of Heat Transfer and Pressure Drop in Helically Micro Finned Tubes

Author

Muhammad Ammar Ali

Registration Number

00000205350

Supervisor

Dr. Muhammad Sajid

DEPARTMENT OF MEHANICAL ENGINEERING

SCHOOL OF MECHANICAL & MANUFACTURING ENGINEERING

NATIONAL UNIVERSITY OF SCIENCES AND TECHNOLOGY

ISLAMABAD

September 2020

Computational Analysis of Heat Transfer and Pressure Drop in Helically Micro Finned Tubes

Author

Muhammad Ammar Ali

Registration Number

00000205350

Supervisor

Dr. Muhammad Sajid

A thesis submitted in partial fulfillment of the requirements for the degree of

MS Mechanical Engineering

Thesis Supervisor:

Dr. Muhammad Sajid

Thesis Supervisor's Signature:

____

DEPARTMENT OF MEHANICAL ENGINEERING

SCHOOL OF MECHANICAL & MANUFACTURING ENGINEERING

NATIONAL UNIVERSITY OF SCIENCES AND TECHNOLOGY

ISLAMABAD

September 2020

FORM TH-4

NATIONAL UNIVERSITY OF SCIENCES AND TECHNOLOGY

MASTER THESIS WORK

We hereby recommend that the dissertation prepared under our supervision by: Muhammad Ammar Ali, 205350. Titled: **Computational Analysis of Heat Transfer and Pressure Drop in Helically Micro Finned Tubes** be accepted in partial fulfillment of the requirements for the award of ____________________degree.

Examination Committee Members

1. Name: Dr. Emad Uddin ____________ Signature:________________

2. Name: Dr. Zaib Ali ____________ Signature:________________

3. Name: Dr. Niaz Bahadur Khan ____________ Signature:________________

Supervisor's name: Dr. Muhammad Sajid ____________ Signature:________________

Date:____________________

________________________ ________________________

Head of Department Date

COUNTERSINGED

Date:__________ ______________

Dean/Principal

Declaration

I certify that this research work titled "*Computational Analysis of Heat Transfer and Pressure Drop in Helically Micro Finned Tubes"* is my own work. The work has not been presented elsewhere for assessment. The material that has been used from other sources it has been properly acknowledged / referred.

Signature of Student

Muhammad Ammar Ali

2017-NUST-MS-Mech-205350

THESIS ACCEPTANCE CERTIFICATE

It is certified that final copy of MS/MPhil thesis written by Muhammad Ammar Ali (Registration No. 00000205350), of SMME has been vetted by undersigned, found complete in all respects as per NUST Statues/Regulations, is free of plagiarism, errors, and mistakes and is accepted as partial fulfillment for award of MS/MPhil degree. It is further certified that necessary amendments as pointed out by GEC members of the scholar have also been incorporated in this dissertation.

Signature: ____________________

Name of Supervisor: Dr. Muhammad Sajid

Date: ____________________

Signature (HOD): ____________________

Date: ____________________

Signature (Dean/Principal): ____________________

Date: ____________________

Plagiarism Certificate (Turnitin Report)

This thesis has been checked for Plagiarism. Turnitin report endorsed by Supervisor is attached.

Signature of Student
Muhammad Ammar Ali

Registration Number # 00000205350

Signature of Supervisor
Dr. Muhammad Sajid

School of Mechanical and Manufacturing Engineering
National University of Science and Technology
Islamabad, Pakistan

Copyright Statement

Acknowledgements

First of all, I am thankful to Allah for guiding me and giving me mental and physical strength to complete this task. Without Him it would never ever be possible to get through the hardships and bottlenecks that I encountered during the course my work.

Secondly, I would like thank my supervisor Dr. Muhammad Sajid for his constant encouragement and guidance. He has taught me what research is and how to go along with it. I have developed very good technical writing skills under his guidance and experience. He never ignored me for any reason whatsoever. I would have given up if it wasn’t for him and I am very thankful for that.

I also am very thankful to Dr. Emad Uddin, Dr. Zaib Ali and Dr. Niaz Bahadur Khan for their guidance and recommendations during my work.

I want to acknowledge the support of my family and friends throughout my research work with their love and affection.

Dedicated to my beloved parents

Abstract

In this study, pressure drop and heat transfer characteristics of smooth tube and internal helically micro-finned tubes with two different fin-to-fin height ratios i.e. equal fin height and alternating fin height, are computationally analysed. The tube with alternating fin height is analysed for proof of concept of pressure drop reduction. Single phase steady turbulent flow model is used with Reynolds number ranging from 12000 to 54000. Water is used as working fluid with inlet temperature of 55°C and constant wall temperature of 20°C is applied. Friction factor, heat transfer coefficient, Nusselt number, and Thermal Performance Index are evaluated and analysed. Numerical results are validated by comparison with the experimental and numerical data from literature. The results showed that the thermal performance is enhanced due to helically finned tube for a range of Reynolds numbers but at the expense of increased pressure drop as compared to smooth tube. The helically finned tube with alternating fin heights showed 5% decrease in friction factor and <1% decrease in heat transfer coefficient as compared with the equal fin heights tube making it a suitable choice for heat transfer applications.

Table of content

List of Figures

List of Tables

Nomenclature

b	fin base width, [m]	P_f	helical Fin pitch, [m]
c	fin top width, [m]	P_b	turbulence kinetic energy due to buoyancy, [J/kg]
$\mathrm{C_p}$	specific heat, [J/kg.K]	P_k	turbulence kinetic energy due to mean velocity gradients, [J/kg]
$\mathrm{C_2}, \mathrm{C_{1\epsilon,}} \mathrm{C_{3\epsilon}}$	User defined constants	Pr	Prandtl number
D	tube diameter, [m]	Re	Reynolds number
e	fin height, [m]	S	strain tensor
E	total energy, [J]	S_h	heat source term, [W/m^2]
f	friction factor	S_k,S_ϵ	turbulence source terms, [J/kg]
$\vec{F}$	external forces, [N]	T	3D temperature array, [K]
$\vec{g}$	gravitational force, [N]	T	temperature, [K]
h	heat transfer coefficient, [W/m^2.K]	U	inlet uniform velocity, [m/s]
h_j	sensible enthalpy, [J]	$\vec{v}$	velocity vector, [m/s]
$\overrightarrow{J_J}$	diffusion flux, [kg/m^2.s]	Y_M	fluctuating dilatation, [J/kg]
K	turbulence kinetic energy, [J/kg]	***Greek Symbols***	
k	thermal conductivity, [W/m.K]	α	helix angle, [deg]
k_{eff}	effective thermal conductivity, [W/m.K]	ϵ	turbulence energy dissipation, [J/kg]
L	tube length, [m]	η	thermal performance index
$\dot{m}$	mass flow rate, [kg/s]	μ	dynamic viscosity, [Pa.s]
N	number of fins	μ_t	Eddy viscosity, [Pa.s]
Nu	Nusselt number	υ	kinematic viscosity, [m^2/s]
P	fluid static pressure, [Pa]	ρ	fluid density, [kg/m^3]
σ_k,σ_ϵ	turbulence Prandtl numbers		
$\bar{\bar{\tau}}$	stress tensor		

Subscripts

b	bulk fluid
finned	finned tube
h	hydraulic
i	inner
in	inlet
o	outer
out	outlet
w	wall

CHAPTER 1: INTRODUCTION

Any place where transfer of heat energy is required, heat exchangers play a major role. They are designed to increase the thermal efficiency of the system. With the development of modern technologies, building compact and lightweight machines have become a common practice. This reduction in size demands innovative solutions for the transfer of energy among the machine components. In case of heat exchangers, a lot research and development is being done to come up with efficient methods for heat transfer. The goal is to develop a method which is thermally and hydraulically efficient and has low production cost.

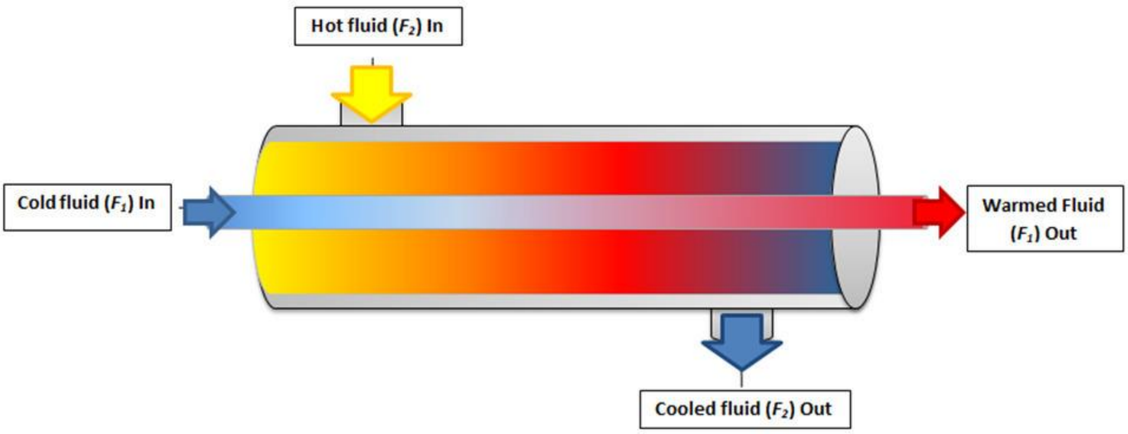

Figure 1: General diagram of a heat exchanger

There are three methods through which heat is transferred from one point to another i.e. conduction, convection and radiation. Radiation requires very high temperatures which is out of the scope of common heat exchanger temperature ranges. Conduction and convection are the two main methods of heat transfer in which convection is the dominant one. Generally, heat exchangers consist of fluids as heat transfer medium. In convection, heat is transferred through thermal diffusion (conduction of heat between fluid particles) which has small contribution and advection (bulk motion of fluid) which has large contribution. So, the main focus when developing heat transfer enhancement technique is to maximize the advection of fluid.

Theoretically you can achieve any desired temperature in heat exchanger with minimum pressure loss by increasing the surface of heat transfer area. But this requires a large size, more material and more weight which is not economic and robust approach. Reducing the size and material demands ingenious methods which can increase the surface to volume ratio and also enhance heat transfer in a smaller area. There are two main techniques through which diffusion and advection in fluids can be increased.

i. Introduction of turbulence in flow
ii. Increasing the surface to volume ratio

Turbulence in a fluid enhances the mixing of fluid enhancing advection. The mixing transports energy from one place to another which creates a difference of energy between two points. This difference maintains the process of heat transfer.

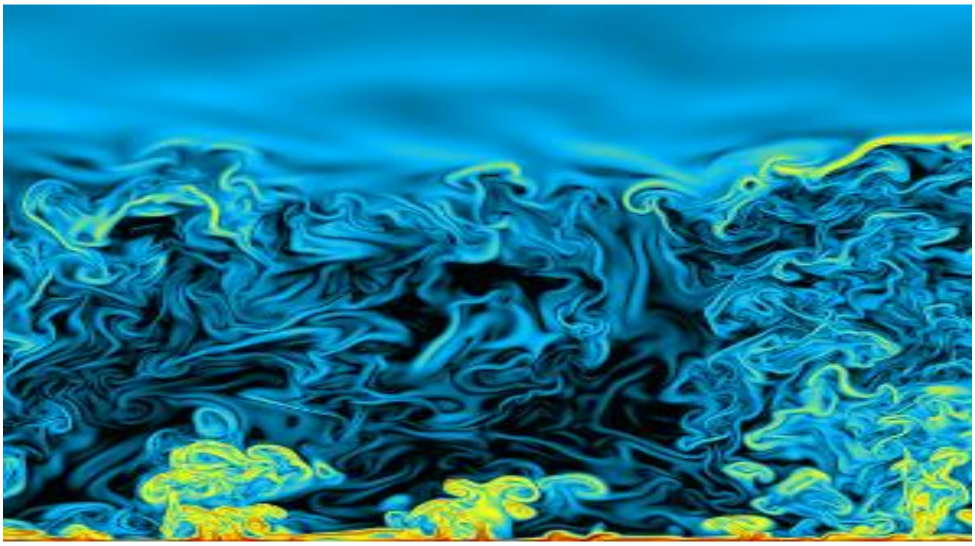

Figure 2: Turbulence in free convection of heat

The conduction of heat between solid and fluid can be increased by increasing the surface area through which heat is being transferred. The more area you have, the more heat you can transfer. But to keep the size of heat exchanger compact, the focus is to increase the surface to volume ratio. Combining the two heat transfer enhancement methods i.e. turbulence and surface to volume ratio, will result in increased thermal performance and decreased overall size of heat exchanger.

A large number of heat transfer enhancement methods have been developed and still new methods are being researched. These methods have been categorized into two main branches.

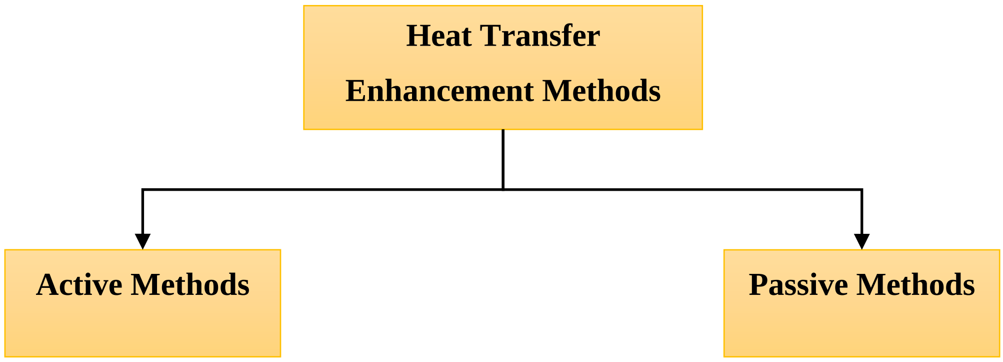

Active methods require external energy source to function whereas passive methods don't require any external energy. Examples of active and passive methods are given below.

Active Methods

i. Electro Hydrodynamics
ii. Jet Impingement
iii. Spray
iv. Surface Vibration
v. Fluid Vibration

Passive Methods

i. Micro fins
ii. Ribs & Grooves
iii. Twisted Tape Inserts
iv. Coiled Wires
v. Porous Medium Inserts
vi. Vortex Generators
vii. Corrugations

Passive methods are more commonly used in industrial applications where as active methods are designed for specific applications. The main purpose of these methods is to increase the surface to volume ratio and introduce turbulence in the flow at the same time [1].

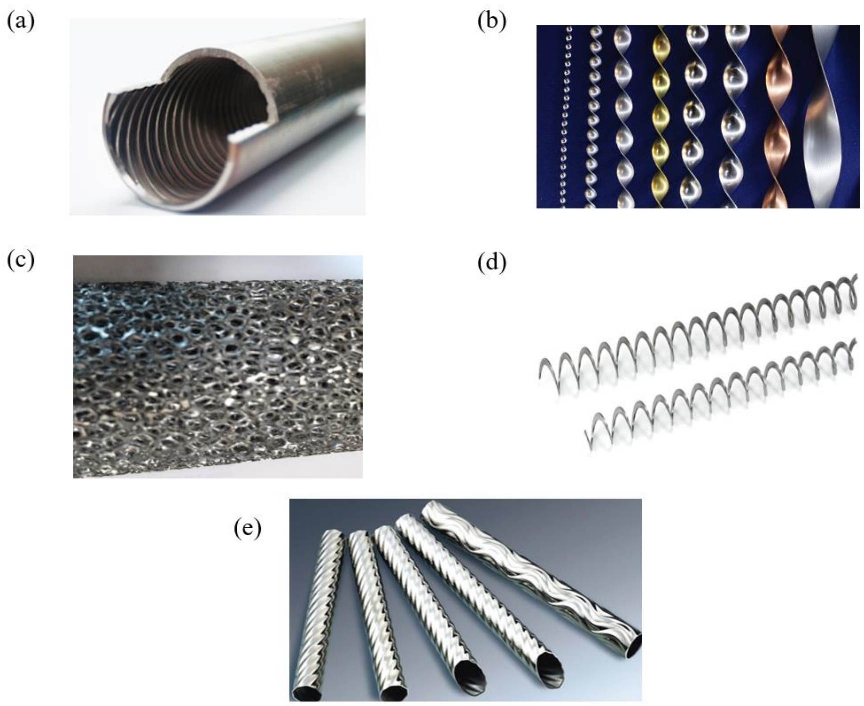

Figure 3: (a) Micro-fins (b) Twisted tape inserts (c) Porous medium insert (d) Coiled wire insert (e) Corrugated tubes

1.1 Literature Review

Due to passive heat transfer methods, the increase in enhanced heat transfer can reach up to six times as compared to the unenhanced one [2]. The drawback of these enhancement techniques is the increase in frictional losses due to turbulence and area increase. This requires a trade-off between desired heat transfer enhancement and pumping power required. Because of higher frictional losses due to pressure drop, extensive research has is being done to find passive methods which will reduce pressure drop as much as possible while increasing the heat transfer as much as possible [3].

To develop such enhancement techniques, researches perform experiments and computational fluid dynamics simulations to understand the flow characteristics of active and passive methods. These experiments and simulations give better understanding of how the fluid is behaving with the introduction of enhancement technique, the flow pattern, physics of energy transfer and the reasons for pressure drop. By gaining knowledge of all these processes, an optimized heat transfer enhancement technique can be developed which will give best performance under applied conditions. A lot of research has been done in understanding flow behavior of active and passive heat transfer methods. We will focus on passive methods because these methods are more common and cost effective. Every technique has its own pros and cons. Literature review shows that passive methods enhance heat transfer with order of magnitude but at the cost of pressure drop. Every passive method is experimentally or computationally investigated by varying different geometrical parameters and flow rates. The thermal and hydraulic flow characteristics are observed for each variable and flow rate and a generalized solution is proposed. The comparison of passive methods is based relative to smooth flow channels. A summary of literature review of passive heat transfer enhancement techniques is given in Table 1.

Table 1: Review of passive heat transfer enchantment techniques

Enhancement Technique	Analysis Technique	Material	Parameters	Observations
Spiral Fin **[4]**	CFD	Water, RT50 (PCM)	Fin thickness, $1.5mm \leq t \leq 2.5mm$ Fin pitch, $10mm < p < 20mm$	Increasing fin pitch reduces melting time by 35% and increasing fin thickness increases melting time by 59%.
Blossom shape internal fins **[5]**	CFD/ Experimental	Air	$3255 \leq Re \leq 19580$ $0.34 \leq P_f/D_h \leq 0.98$ $0.78 \leq e/D_h \leq 1.51$	Heat transfer performance of 3- and 4-pieces blossom fin is greater than 2-pieces blossom fin. Numerical correlation had a mean deviation of 8.69% in *Nu* and 6.76% in *f*.
Arc shape fins with Y-shape inserts **[6]**	Experimental	Water	$4108 \leq Re \leq 14500$ $e = 0.7mm$, $P_f = 0.6mm$,Y-insert L = 30.5mm	*Nu* is 2.1~4.3 times higher than smooth tube. *f* is 6.89~9.25 time more than smooth tube. Overall thermal performance is 1.02~2.22 times more than smooth tube.
Internal repeated ring ribs **[7]**	CFD	Air	$3600 \leq Re \leq 16500$ $0.29 \leq P_f/D_i \leq 4.35$ $0.025 \leq e/D_i \leq 0.069$	Highest *Nu* was obtained using ring type ribs as compared to other rib geometries. *Nu* was within ±10%, *f* within ±15% and performance evaluation criterion was within ±15% of experimental results.
Dimples **[8]**	Experimental	Water, R-134a	$300 \leq$ Mass flux[$kg.m^{-2}.s^{-1}$] ≤ 500 $10 \leq$ Heat flux[$kW.m^{-2}$] ≤ 20 0.5mm ≤Dimple depth≤ 1.0mm	83% and 893% increase recorded in heat transfer coefficient and friction factor respectively. The efficiency index is less than 1 for all configurations, which limits the use of dimpled tubes for special applications.

Dimples & longitudinal grooves **[9]**	Experimental	Water, R-410a	$70 \leq$ Mass flux[$kg.m^{-2}.s^{-1}$] ≤ 150 $32.6 \leq$Heat flux[$kW.m^{-2}$] ≤ 37 Groove pitch = 3.4mm	Enhanced tubes increase the heat transfer coefficient with increasing mass flux. At constant mass flux, heat transfer coefficient increases by increasing heat flux.
Twisted tape inserts **[10]**	Experimental	Water	$400 \leq$ Re ≤ 11400 $2 \leq$Heat flux[$kW.m^{-2}$] ≤ 4 $3 \leq$Twist ratio≤ 5	As the twist ratio decreased, the Colburn j-factor increased and caused early transition. Increasing twist ratio decreased the friction factor.
Twisted tape inserts **[11]**	Experimental	R-134a	$75 \leq$ Mass flux[$kg.m^{-2}.s^{-1}$] ≤ 1000 $5 \leq$Heat flux[$kW.m^{-2}$] ≤ 250 $3 \leq$Twist ratio≤ 14	Twisted inserts increased heat transfer by causing earlier transition to turbulent flow. Mass fluxes higher than 400 and heat fluxes higher than 100 caused no change in heat transfer coefficient. Improvements in heat transfer were measured for low to moderate mass and heat fluxes.
Annular metal foam inserts **[12]**	Experimental	Water	$20 \leq$ Vapor mass-flow rate [$kg.h^{-1}$] ≤ 100 $1 \leq$ Water flow rate [$m^3.h^{-1}$] ≤ 3	Heat transfer unit mass efficiency coefficient is 1.3 times greater than the corresponding micro-fin tube. Increasing metal foam size, increases the pressure drop.
Metallic foam, circumferential pin fins, twisted pin fins **[13]**	Experimental	R-134a	$50 \leq$ Mass flux[$kg.m^{-2}.s^{-1}$]≤ 150 Saturation pressure = 11.6 bar, 13.4 bar	Average increase in heat transfer coefficient for the enhanced tubes is 2 times the plain tube. Head impact flow configuration for eight-fin tube is measured to be the best.
Twisted tape inserts **[14]**	Experimental	R-1234yf	$160 \leq$ Mass flux[$kg.m^{-2}.s^{-1}$] ≤ 310 $6 \leq$ Twist ratio ≤ 12	42% and 235% increase in heat transfer coefficient and pressure drop measured as compared to smooth tube.
Delta winglet vortex generator **[15]**	Experimental	Water	$5000 \leq$ Re ≤ 25000 Winglet height = 5mm, 7.5mm and 10mm	*Nu* and *f* increase by increasing winglet height and attack angle.

				Maximum of 73% increase in *Nu* and 2.5 times higher *f* is measured as compared to smooth tube.
Micro-finned tube **[16]**	CFD	Oil	$100 \leq Re \leq 1000$ 0.2mm < e < 0.5mm, 5º < α < 45º	44% increase in heat transfer and 69% increase in friction factor at 1000 Re.
Micro-finned tube **[17]**	Experimental	Water/ CuO nanofluid	$5650 \leq Re \leq 17000$ $P_f/D_i = 0.05$ $e/D_i = 0.019$	*Nu* and *f* increased by 1.5 times and 2 times respectively as compared to plain tube. η was observed to be more than unity across the whole range of *Re*.
Micro-finned tube **[18]**	Experimental	Water	$5725 \leq Re \leq 25353$ $P_f/D_i = 0.045$, $e/D_i = 0.027$	Pressure drop measured on average to be 2 times more than the smooth tube.
Micro-finned tube **[19]**	Experimental	Water	$8000 \leq Re \leq 24000$ $e/D_i = 0.020$	Heat transfer coefficient increased 33% as compared to smooth tube
Helical Groove **[20]**	CFD	Water	$4000 \leq Re \leq 20000$ 7.1mm < Groove Pitch < 305mm	Maximum η of 1.2 achieved at Re 15000 and pitch length of 130mm.
Micro-finned tube **[21]**	Experimental	Water	$10000 \leq Re \leq 70000$ 0.007mm < e/D_i < 0.085mm, 0º < α < 45º	Increase in *Nu* was measured 15-180% and *f* 50-500% more than the smooth tube.
Micro finned tube **[22]**	Experimental	Water	$2300 \leq Re \leq 20000$ $P_f/D_i = 0.052$, $e/D_i = 0.022$	Heat transfer coefficient increased 2.9 times and pressure drop increased 1.7 times as compared to smooth tube for Re >10000.
Micro-finned tube **[23]**	Experimental	Water	$3000 \leq Re \leq 40000$ 0.12mm < e < 0.15mm, 9º < α < 25º	Maximum η calculated was 1.35 for *Re* ≈10000 η became less than unity for Re > 30000
Micro-finned tube **[24]**	Experimental	Water, Oil	$2500 \leq Re \leq 90000$ $e/D_i = 0.017$	Heat transfer coefficient more than twice that of the smooth tube. Friction factor 40-50% more than that of the smooth tube.
Micro-finned tube **[25]**	Experimental	Water	$12000 \leq Re \leq 60000$ 0.0199mm < e/D_i < 0.0327mm, 25º < α < 48º	Highest Colburn j-factor achieved for tube with N= 45, α = 48º, $e/D_i = 0.0244$. Lowest friction factor achieved for tube with N= 10, α = 48º, $e/D_i = 0.0244$.

Micro-finned tube, Corrugated tube **[26]**	CFD	Water	$12000 \leq Re \leq 57000$ $e/D_i = 0.024mm$, $25^o < \alpha < 48^o$	Highest heat transfer coefficient and friction factor obtained for $N= 45$, $\alpha = 48^o$, $e/D_i = 0.024$. Corrugated tubes showed intermediate performance between smooth and finned tubes.
Longitudinal finned tube **[27]**	Experimental	Fe_3O_4, Water	$5300 \leq Re \leq 49200$ $e/D_i = 0.15mm$	Heat transfer increase of 80-90% observed as compared to plain tube. Friction factor increased 3-4 times as compared to plain tube.
Micro-finned coiled tube **[28]**	Experimental	R-134a	$75 \leq$ Mass flux [kg m^{-2} s^{-1}] ≤ 191 $e/D_i = 0.02mm$, $\alpha = 18^o$	Coiled micro-finned tube showed 160-255% and 69-155% higher heat transfer coefficient and pressure drop respectively, as compared to straight smooth tube.
Micro-finned tube with porous copper fiber insert **[29]**	Experimental	Water	$4000 \leq Re \leq 14000$ $e/D_i = 0.052mm$	Heat transfer coefficient increase measured 6.4 times than that of smooth tube. η value of 2.29 evaluated.
Micro-finned tube **[30]**	Experimental	R410A	$100 \leq$ Mass flux [kg m^{-2} s^{-1}] ≤ 450 $e/D_i = 0.033mm$	Heat transfer coefficient and pressure drop increased on average of 1.34 and 1.23 times respectively as compared to the smooth tube.

1.2 Scope of Work

From literature review, it can be observed that micro-finned tubes have relatively good overall thermohydraulic performance. They are widely used in practical applications due to low production cost, relatively lower pressure losses and stable performance in the long run [2].

In this study, computational fluid dynamics analysis of heat transfer and pressure drop in helically micro-finned tubes is performed under varying Reynolds number. Computational analysis is carried out using commercially available CFD software ANSYS Fluent. Two types helically micro-finned tube geometries have been analyzed with fin-to-fin height ratio of 1:1 and 1:2. The 1:2 shows here that fin height alternates with one fin being half in height of the other. Throughout the document, the equal fin height tube will be represented as 1:1 tube and alternating fin height tube as 1:2 tube. A lot of literature is available on equal fin height micro-finned tubes but not enough research is available on alternating fin height tubes. The idea of alternating fin height is being introduced here to study its effect on the pressure drop because that is main drawback of passive methods. Also, a smooth tube with the same length and diameter as micro-finned tubes is analyzed to serve as reference for the relative thermal and hydraulic performance. The geometrical parameters of the micro-finned tubes are taken from the experimental thermal and hydraulic analysis of micro-finned performed by [25]. In their experiment, the authors used a double pipe counterflow heat exchanger with test tube on the inside. The test tube had helical micro fins on both internal and external surfaces. The test tube contained the hot fluid and the cold fluid ran in the annulus. Only the test tube side was chosen for this study as fluid domain for the computational analysis with micro fins only on the inner surface. This was done to simplify the geometry because of the limited computational resource. As this study is a comparative analysis between three tubes, so the effect of simplification in fluid domain will be balanced out. Another reason for simplification was to validate the results with the computational analysis of [26] which used the same fluid domain as in this study.

CHAPTER 2: COMPUTATIONAL METHODOLOGY

Thermal and hydraulic flow analysis of helically finned tubes and smooth tube are investigated computationally using ANSYS Fluent CFD. The first step in any CFD simulation is to determine the problem definition. For problem definition, you need to answer the following questions,

i. What is it that you want to simulate?
ii. What are the results that you want to achieve?
iii. Is the flow single phase or multi-phase?
iv. Do you want to do steady or transient analysis?
v. Is the flow regime laminar or turbulent?
vi. Is it an external or internal flow?
vii. Is the fluid compressible or incompressible?

The current study is single phase, steady, turbulent, internal and incompressible CFD analysis. After answering these questions, an iterative process starts in which the fluid domain is selected, the model is built, then grid/mesh is formed and after that boundary conditions and computational solution is run on the generated grid/mesh. The flowchart of computational analysis is given in Fig. 4.

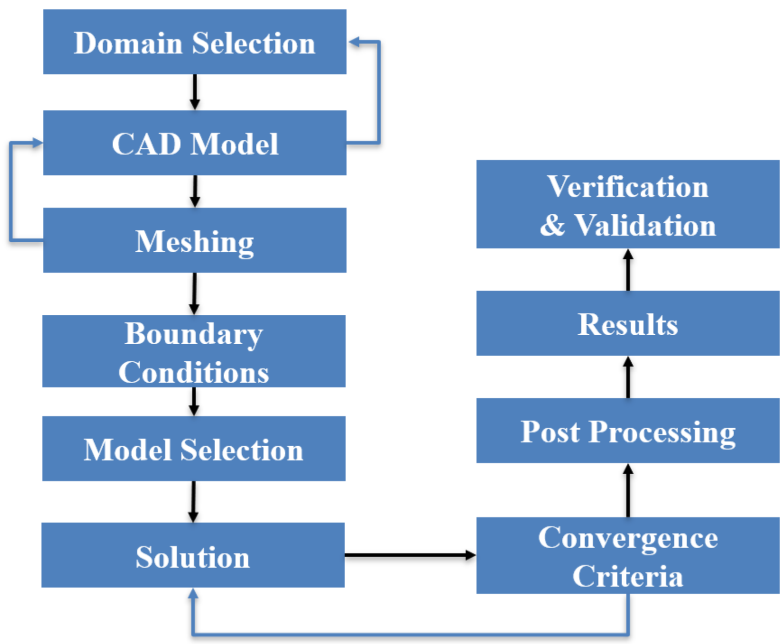

Figure 4: Flowchart of computational methodology

2.1 Domain Definition

The geometrical specifications of the fluid domain for the micro-finned tubes and smooth tube are presented in Tab. 2. 3D CAD model geometry along with cross- section of the tubes is shown the Fig. 5.

Table 2: Geometric parameters of fluid domain

Parameters	L [m]	D_o [m]	D_i [m]	e [m]	b [m]	c [m]	α [deg]	P_f [m]	N	$\frac{e}{D_i}$
Smooth	2.74	0.0188	0.0156	--	--	--	--	--	--	--
1:1 tube	2.74	0.0188	0.0156	3.8×10^{-4}	4.8×10^{-4}	2.0×10^{-4}	25	0.102	10	0.024
1:2 tube	2.74	0.0188	0.0156	1.9×10^{-4} 3.8×10^{-4}	4.8×10^{-4}	2.0×10^{-4}	25	0.102	10	0.012-0.024

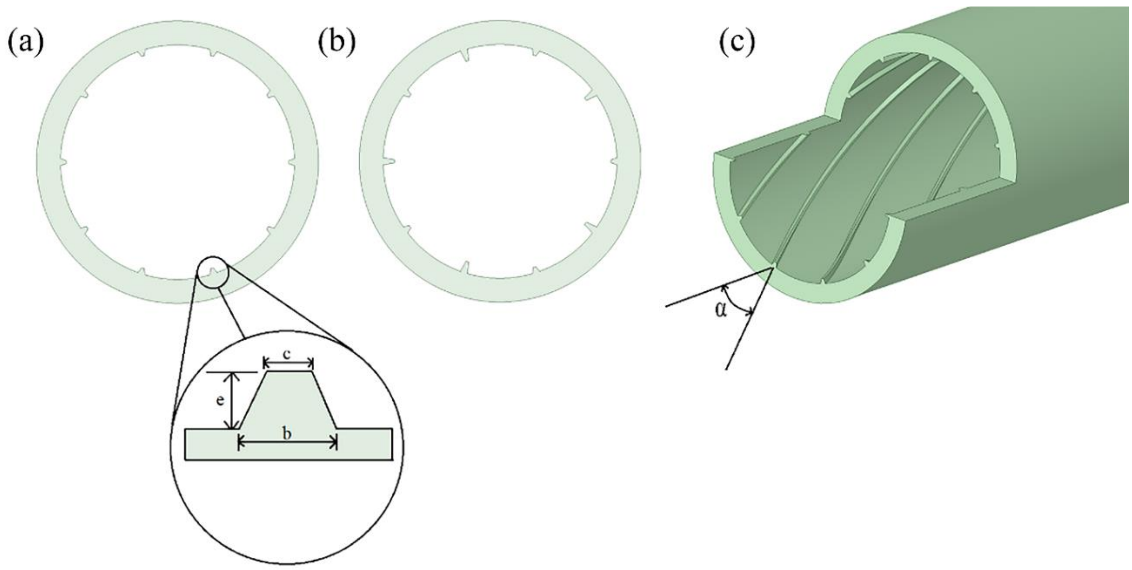

Figure 5: Helically finned tube geometry, (a) Equal fin height tube cross-section (b) Alternating fin height tube cross-section (c) 3D tube geometry

The geometry is helically symmetric which can be utilized to select only a sector of the whole domain for numerical computation. For this reason, a helically symmetric sector of the tube is chosen as the fluid domain reducing the grid size and computational time. The CAD model of fluid domain and tube sector cross-section are shown in Fig. 6.

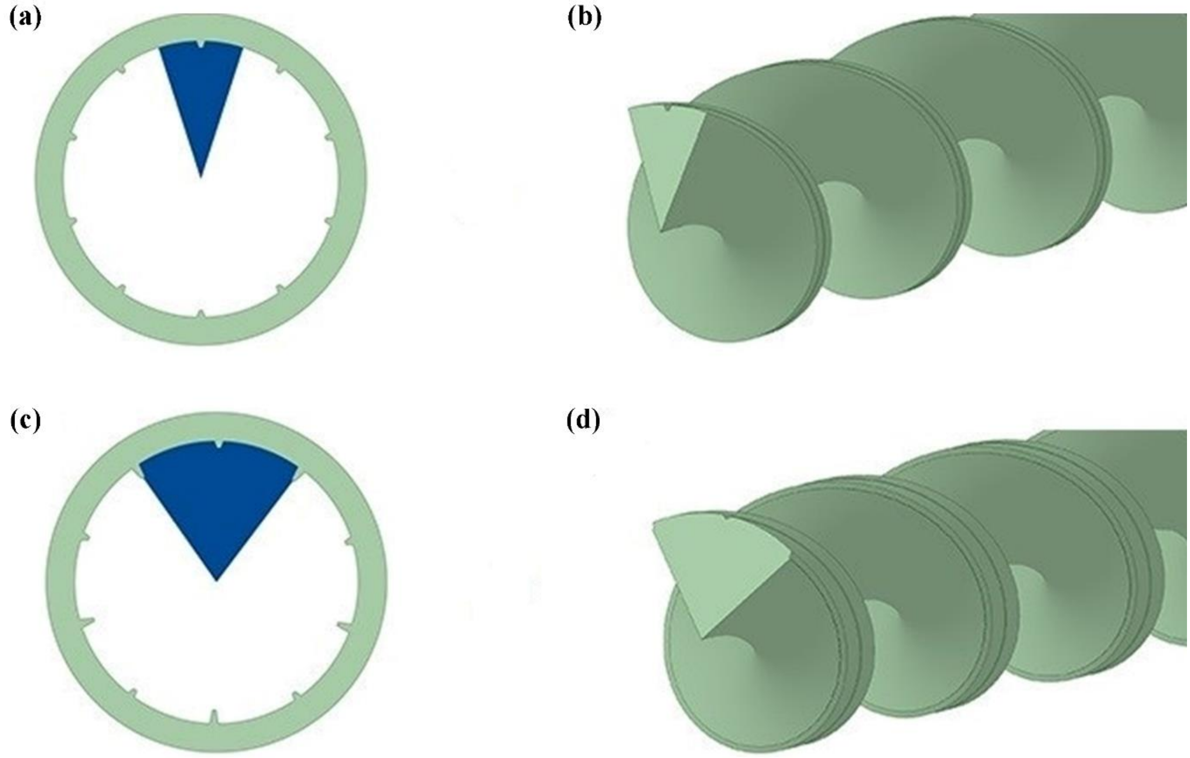

Figure 6: Fluid domain CAD model and sector cross-section geometry (a) Equal fin height sector (b) Equal fin height fluid domain (a) Alternating fin height sector (b) Alternating fin height fluid domain

2.2 Meshing and Boundary Conditions

The meshing of the model was done in ANSYS Fluent using sweep meshing algorithm with local mesh controls on the edges. The mesh was kept fine at the fin edges because this is the critical area where rapid changes in the flow will occur. Mesh grid is shown in Fig. 7 for both micro-finned tubes.

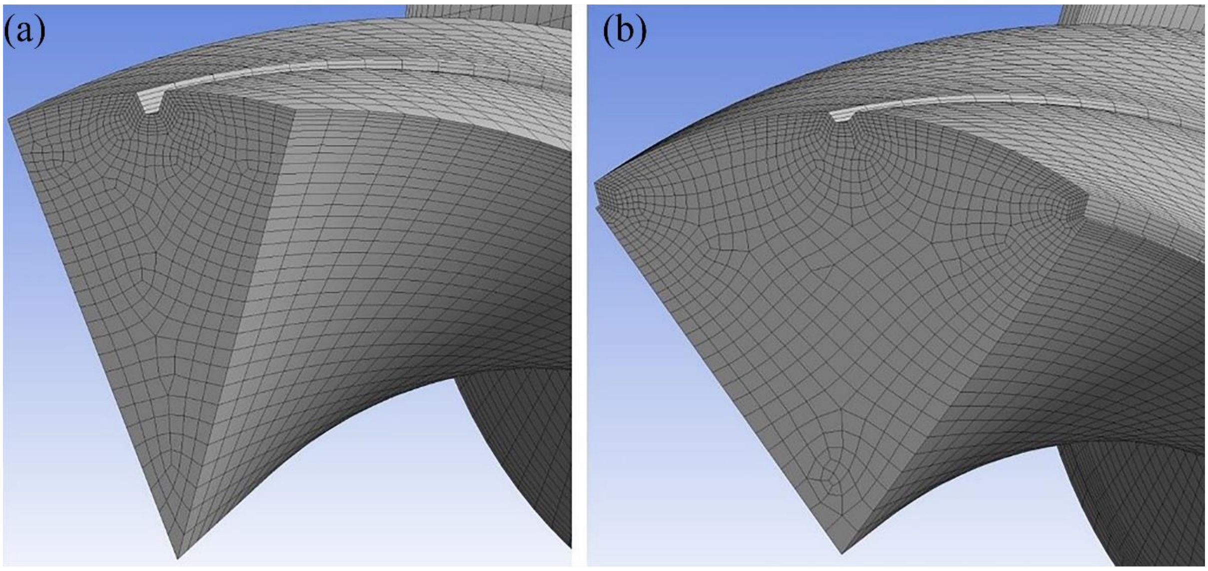

Figure 7: Mesh grid of fluid domain sector (a) Equal fin height, (b) Alternating fin height

Three different meshes were generated for each tube for grid independence study. Mesh quality parameters are given in Table. 3.

Table 3: Mesh quality parameters

Pipe Geometry	Cell Count	Orthogonality	Skewness	Aspect Ratio
1:1	1,627,560	0.87	0.28	10.5
1:2	2,800,280	0.88	0.27	11.0
Smooth	594,580	0.96	0.17	4.8

Water with uniform velocity and temperature of 55°C enters the tube and constant temperature of 20°C is applied as boundary condition to the wall of the tube. Due to symmetry of the fluid domain, rotational symmetric boundary conditions is applied on the side faces. Figure 8 shows visualization of boundary conditions on the fluid domain and Table 4 gives summary of boundary conditions applied at each face.

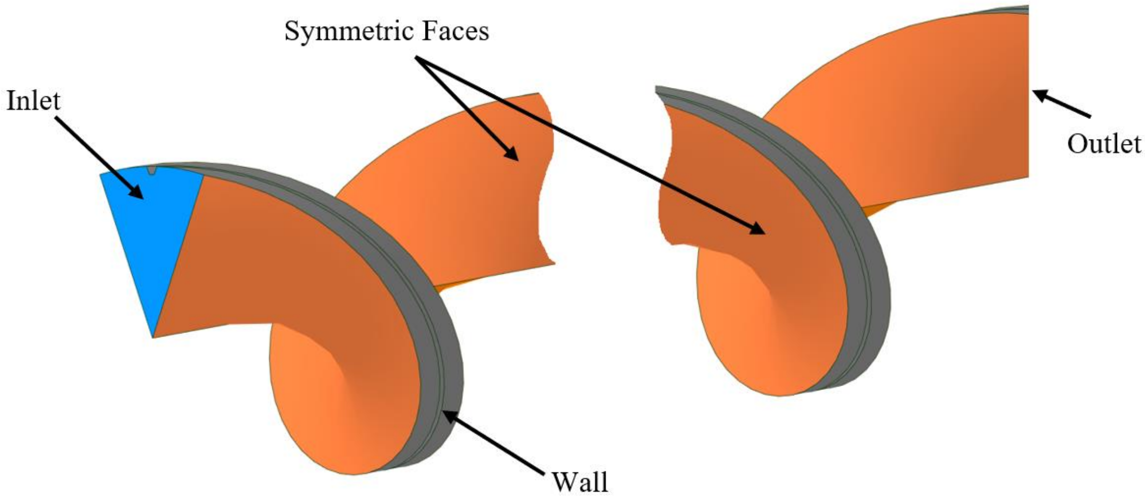

Figure 8: Boundary conditions on fluid domain

Table 4: Flow boundary conditions

Boundary	Hydraulic BC	Thermal BC
Inlet	Uniform Inlet Velocity Re: 12000-54000	Constant Temperature 55°C
Outlet	Pressure Outlet (Zero Gauge Pressure)	Program Controlled
Wall	No Slip	Constant Temperature 20°C
Side Faces	Rotational Periodic BC	

2.3 Governing Equations and Turbulence Model Selection

From the literature review it was observed that for the micro fin and related geometries, the best turbulence model which gives accurate results is the Realizable K-ε model. The Realizable model improves the standard K-ε model by incorporating effects of separating and swirling flows, both of which are observed in micro finned tube flow. For the current study, Realizable K-ε model was chosen with enhanced wall function to accurately model the flow in sub-laminar and buffer layer with moderate near wall mesh density. The enhanced wall function does not require a very dense mesh near wall with very small first layer height. Apart from conservation of continuity and momentum equations, two equations for turbulence modeling and energy equation are solved. Following are governing equations for the steady turbulent flow with heat transfer [31],

Continuity Equation:

$$\nabla.(\rho.\vec{v}) = 0 \tag{1}$$

Momentum Equation:

$$\nabla.(\rho\vec{v}\vec{v}) = -\nabla \mathrm{P} + \nabla.\bar{\bar{\tau}} + \rho\vec{g} + \vec{F} \tag{2}$$

Energy Equation:

$$\nabla.\left(v(\rho E + \mathrm{P})\right) = \nabla.\left(k_{eff}\nabla T - \sum_j h_j \vec{J_j} + (\tau_{eff}.v)\right) + S_h \tag{3}$$

Realizable K-ε Turbulence Model:

$$\frac{\partial}{\partial x_j}(\rho K u_j) = \frac{\partial}{\partial x_j}\left[\left(\mu + \frac{\mu_t}{\sigma_k}\right)\frac{\partial K}{\partial x_j}\right] + P_k + P_b - \rho\epsilon - Y_M + S_k \tag{4}$$

$$\frac{\partial}{\partial x_j}(\rho \epsilon u_j) = \frac{\partial}{\partial x_j}\left[\left(\mu + \frac{\mu_t}{\sigma_\epsilon}\right)\frac{\partial \epsilon}{\partial x_j}\right] + \rho C_1 S\epsilon - \rho C_2 \frac{\epsilon^2}{\mathrm{K} + \sqrt{\nu\epsilon}} + C_{1\epsilon}\frac{\epsilon}{K}C_{3\epsilon}P_b + S_\epsilon \quad (5)$$

$$C_1 = \max\left[0.43, \frac{\eta}{\eta+5}\right], \quad \eta = S\frac{K}{\epsilon}, \quad S = \sqrt{2S_{ij}S_{ij}}$$

The constants of the equations are given by [31].

$$C_{1\epsilon} = 1.44, C_2 = 1.9, \sigma_k = 1.0, \sigma_\epsilon = 1.2$$

2.4 CFD Solution Algorithm

The Coupled solution algorithm is chosen because it provides accurate results for turbulent single-phase steady-state flows. Because all the governing equations are solved simultaneously in this method, therefore, the convergence rate is faster as compared to pressure-based segregated algorithm but at the expanse of computational cost.

2.4.1 Data Reduction

Fanning friction factor, heat transfer coefficient, Nusselt number and thermal performance index were calculated by using relationships from [16],

$$f = \frac{\Delta P D_h}{2L\rho U^2} \quad (6)$$

Fanning friction factor is calculated from the pressure field generated by the numerical solver.

$$h = \frac{\dot{m}c_p}{\pi D_i L} \frac{(T_{out} - T_{in})}{(T_w - T_b)} \tag{7}$$

Equation (7) calculates the overall heat transfer coefficient using average values of temperature at the inlet and outlet of fluid domain. Equation (8) determines Nu from heat transfer coefficient, hydraulic diameter and thermal conductivity.

$$Nu = \frac{hD_h}{k} \tag{8}$$

$$\eta = \frac{h_{finned}/h_{smooth}}{f_{finned}/f_{smooth}} \tag{9}$$

Equation (9) is used to calculate thermal performance index which determines the overall thermohydraulic performance of the system.

CHAPTER 3: RESULTS AND DISCUSSION

In order to improve thermohydraulic performance of heat exchangers, passive cooling techniques provide an overall good solution. These techniques make use of both the surface area increase and flow disturbance for heat transfer enhancement. Normally micro-finned tubes with equal fin heights are common in heat exchanger applications. In this study helical micro-finned tubes with same and alternating fin heights are numerically investigated to analyses the comparative thermohydraulic performance.

3.1 Grid Independence Study

A grid independence study was carried out to analyze the variation of friction factor and heat transfer coefficient with increasing grid size. Three grid sizes were chosen for both the micro-finned tubes. The plots show no significant improvement in flow characteristics with increasing grid size. Therefore, grid size of 1600000 and 2800000 elements were chosen for equal fin height tube and alternating fin height tube respectively.

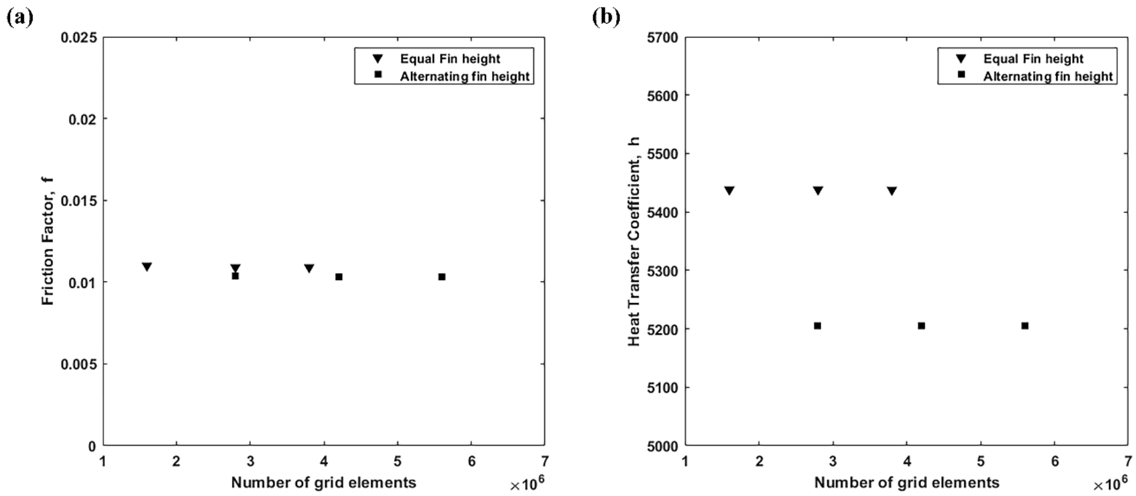

Figure 9: Grid size dependence of (a) friction factor (b) heat transfer coefficient

3.2 Numerical Procedure Validation

The results obtained from numerical simulations for the studied tubes were compared with the experimental results from [25]and numerical results from [26]. They used eight different micro-finned tubes and a smooth tube and measured pressure drop and heat transfer characteristics for a range of Reynolds numbers. In the current study only one of micro-finned tube and smooth tube from experimental study were chosen for numerical simulation. Comparison of friction factor between current study and experimental results is shown in Fig. 10.

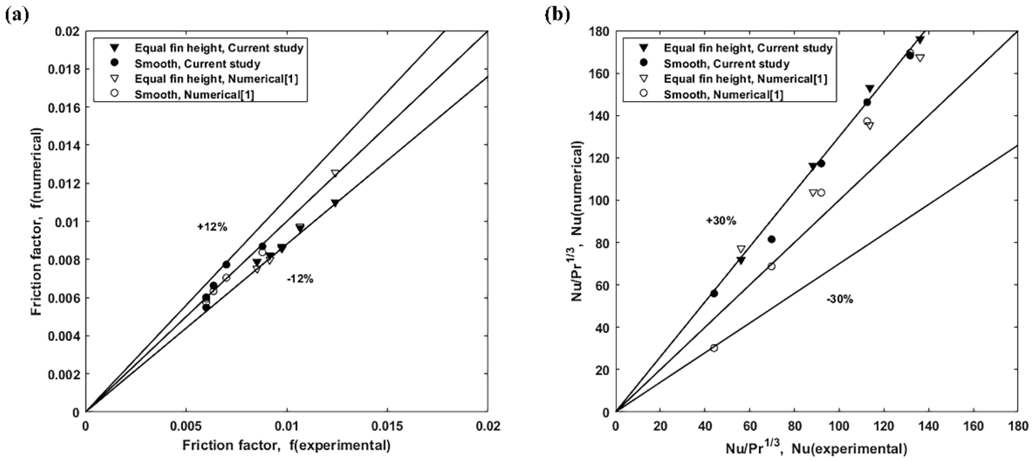

Figure 10: Validation of results with experimental and numerical data from literature,(a) friction factor (b) Scaled Nu

The friction factor obtained from numerical results shows good agreement with the experimental and numerical results for both the smooth and micro-finned tube. The numerical results remain within ±12% of the experimental results validating the numerical procedure. The scaled Nu deviates about ±14% from experimental results but shows a good agreement with the numerical results performed by [26] using the same micro-finned tube geometry and boundary conditions. This deviation is due to the simplified fluid domain and boundary conditions selection.

3.3 Effect of Micro Fins on Pressure Drop and Heat Transfer

The inclusion of micro fins in tube flow increases the heat transfer by introducing flow disturbances e.g. rotations and turbulence. But this also increases the resistance to flow causing more pressure drop. The goal is to increase the heat transfer while keeping the pressure drop under acceptable levels. For carrying out the comparative analysis of pressure drop and heat transfer characteristics of the micro-finned tubes, numerical simulation were performed for Re ranging from 12000 to 54000. All the simulations were performed under steady state using turbulence modeling. Temperature contours at the outlet cross-section for Reynolds number 12000 and 54000 are given in Fig. 11.

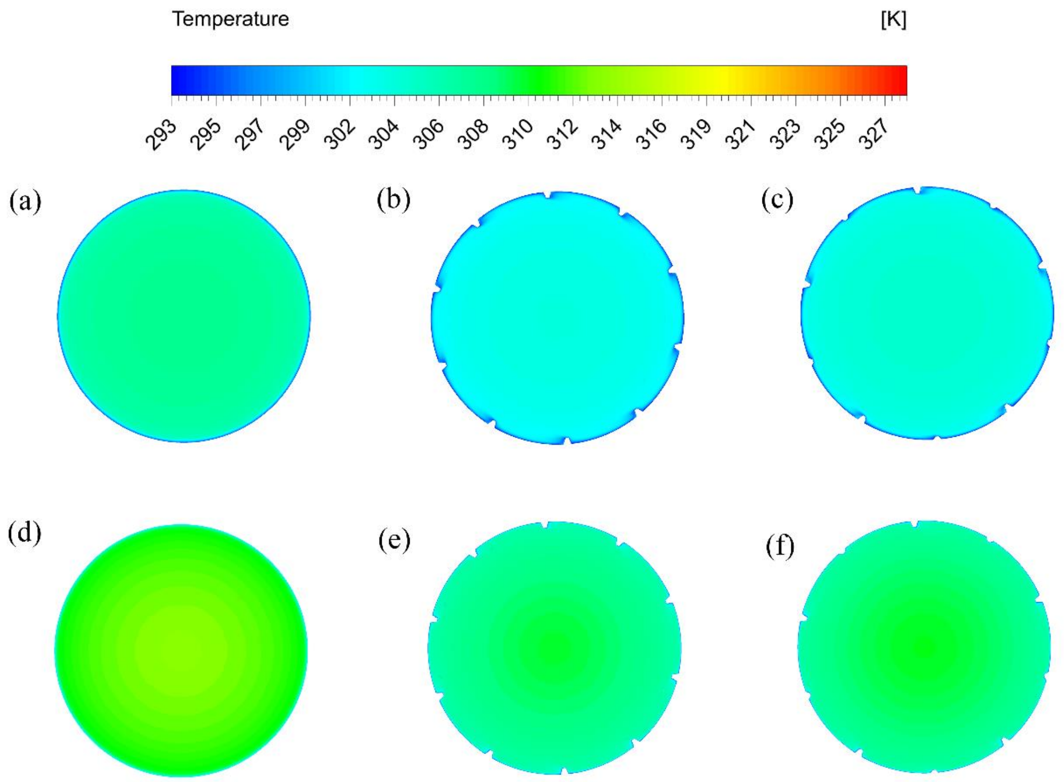

Figure 11: Temperature contours at outlet cross-section (a) Smooth tube, Re 12000 (b) Fin-to-Fin height 1:1, Re 12000 (c) Fin-to-Fin height 1:2, Re 12000 (d) Smooth tube, Re 54000 (e) Fin-to-Fin height 1:1, Re 54000 (f) Fin-to-Fin height 1:2, Re 54000

Temperature contour plots show that as the Re number increases, the temperature drop becomes less and less which agrees with the theory. The finned tubes have higher temperature drop as compared to smooth tube. Both the helically finned tubes show relatively similar temperature drop at the outlet as the Re increases. This shows that the finned tube with fin-to-fin height ratio of 1:2 is a promising solution for heat transfer enhancement. Pressure contours of the three studied tubes for Re 12000 and 54000 at the inlet cross-section are given in Fig. 12.

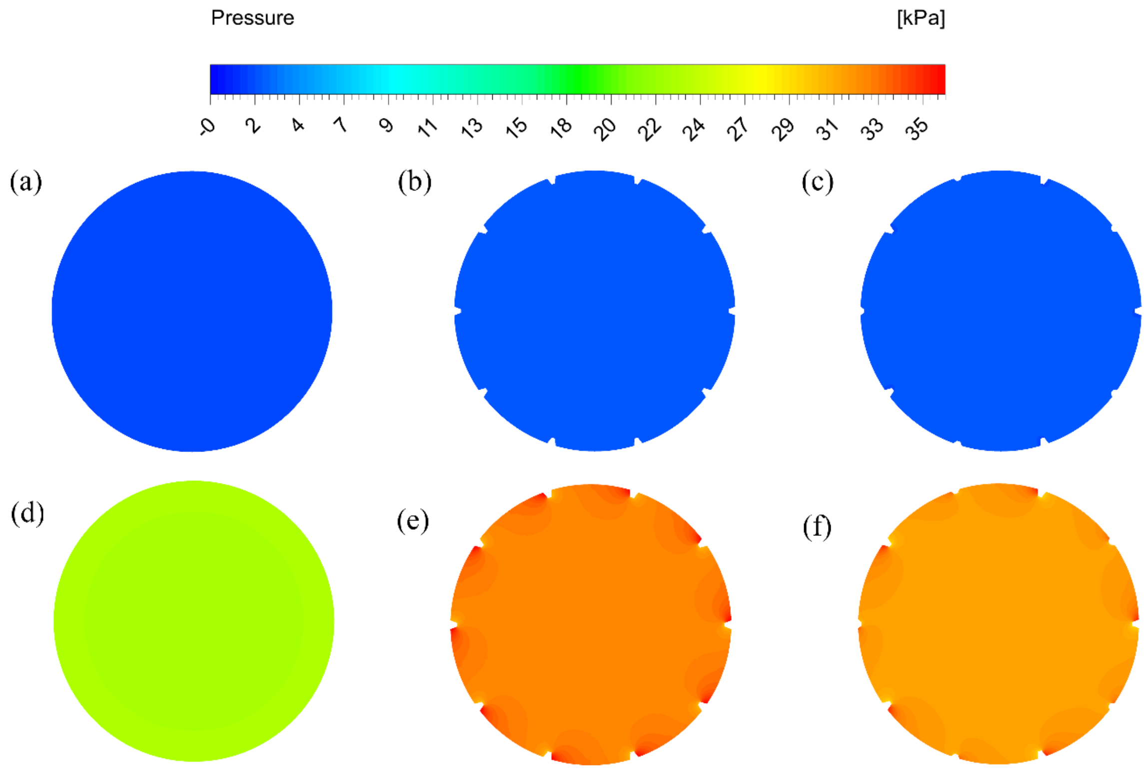

Figure 12: Pressure contours at inlet cross-section (a) Smooth tube, Re 12000 (b) Fin-to-Fin height 1:1, Re 12000 (c) Fin-to-Fin height 1:2, Re 12000 (d) Smooth tube, Re 54000 (e) Fin-to-Fin height 1:1, Re 54000 (f) Fin-to-Fin height 1:2, Re 54000

The contours clearly show that the pressure drop for helically finned tube with fin-to-fin height ratio of 1:2 is relatively less than the tube with fin-to-fin height ratio of 1:1. This indicates a better hydraulic performance for the fin-to-fin height ratio of 1:2. Keeping in view that the temperature drop for both helically finned tubes was almost similar. Both these results indicate fin-to-fin height ratio of 1:2 has relatively better performance in terms of pumping power required to obtain the heat transfer enhancement.

Using the post processing techniques, we can analyse the flow pattern and its changing behaviour by visualizing the streamlines. Visualization of flow will give us a clear understanding of how the micro fins enhance the heat transfer. Figure 13 shows the velocity streamlines at the half length cross-section of both the micro-finned tubes. The colour spectrum of streamlines shows the strength of local vorticity introduced due to micro fins. The vorticity effects are local to micro fins. Therefore, for better visualization the seeding of streamlines is only done locally near the micro fins.

(a)

(b)

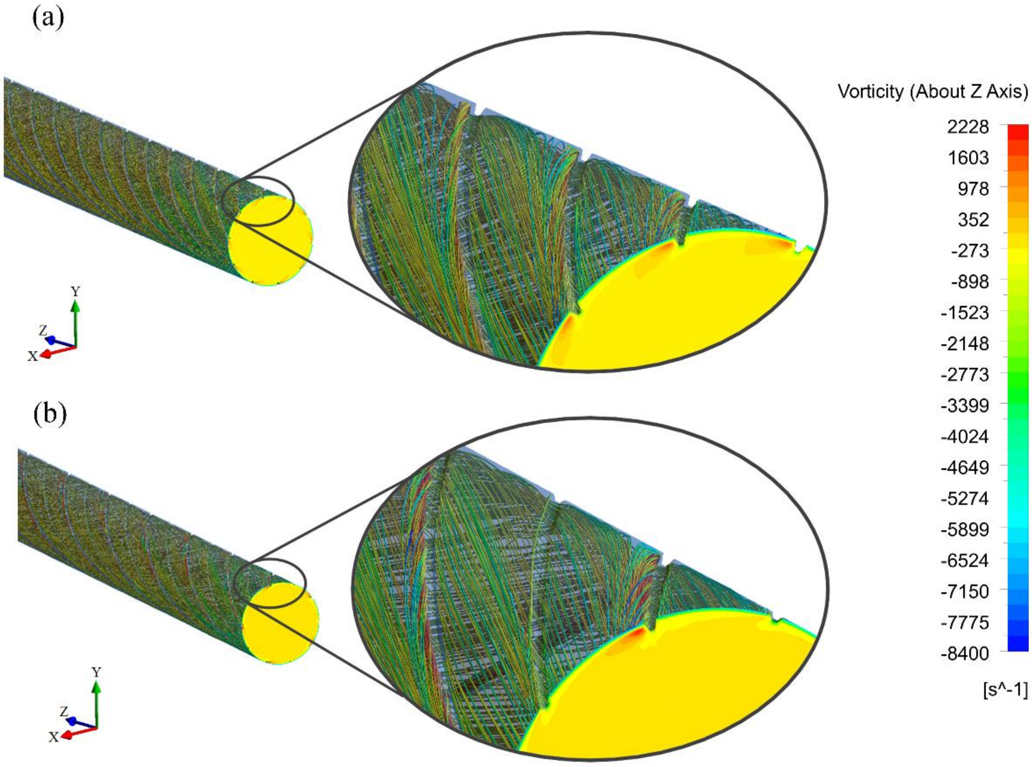

Figure 13: Velocity streamlines with overlaid vorticity contours for (a) equal fin height tube (b) alternating fin height tube

We can see the local rotation of fluid velocity streamlines along the boundary of micro fins showing the strength of vorticity. These local rotations cause the mixing of fluid and hence enhance the heat transfer between wall and the fluid. On the other hand, these rotations are what causing increased pressure drop also along with the resistance offered by the micro fin geometry. In comparison, both the micro-finned tubes show the presence of local vorticity in flow which is the indication of their relatively similar heat transfer coefficient. In case of pressure drop, the equal fin height tube shows relatively higher values as compared to alternating fin height tube.

When the Re is low, the flow in both micro finned tubes remains attached to the wall even though the micro fins have significant effect on the introduction of turbulence. The strength of turbulence kinetic energy is higher in 1:1 tube as compared to 1:2 tube due to which the heat transfer and pressure drop is higher. The heat is being transferred to the wall from hot fluid in two ways. First there is turbulence which transfers heat to the wall from rest of the fluid and second is the heat transfer in the vicinity of wall through the attached flow. When Re is small, the heat is being transferred through both ways in micro finned tubes. Because the turbulence kinetic energy is higher in 1:1 tube, therefore, the heat transfer is higher. At higher Re, the flow separates from the wall in 1:1 tube due to very high turbulence kinetic energy but it still remains attached to the wall in case of 1:2 tube because of the smaller height of half of fins. So now less heat is being transferred in 1:1 due to separation of flow from the wall as compared to 1:2 tube. But the turbulence kinetic energy is still much higher in 1:1 tube. So, the overall heat transfer is balanced in both micro finned tubes at higher Re. That's why the temperature drop is almost equal in micro finned tubes at higher Re. Figures 14 and 15 show the effect of turbulence kinetic energy on the attachment and detachment of flow in micro-finned tubes.

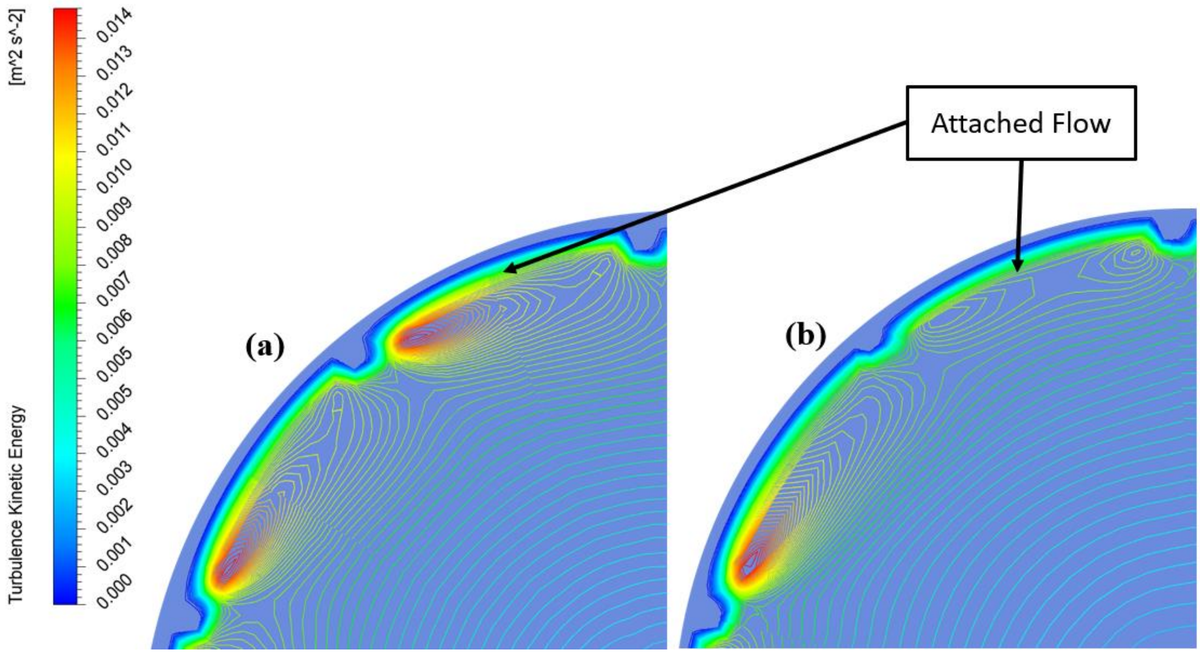

Figure 14: Turbulence kinetic energy contours at Re 12000 for (a) Equal fin height (b) Alternating fin height

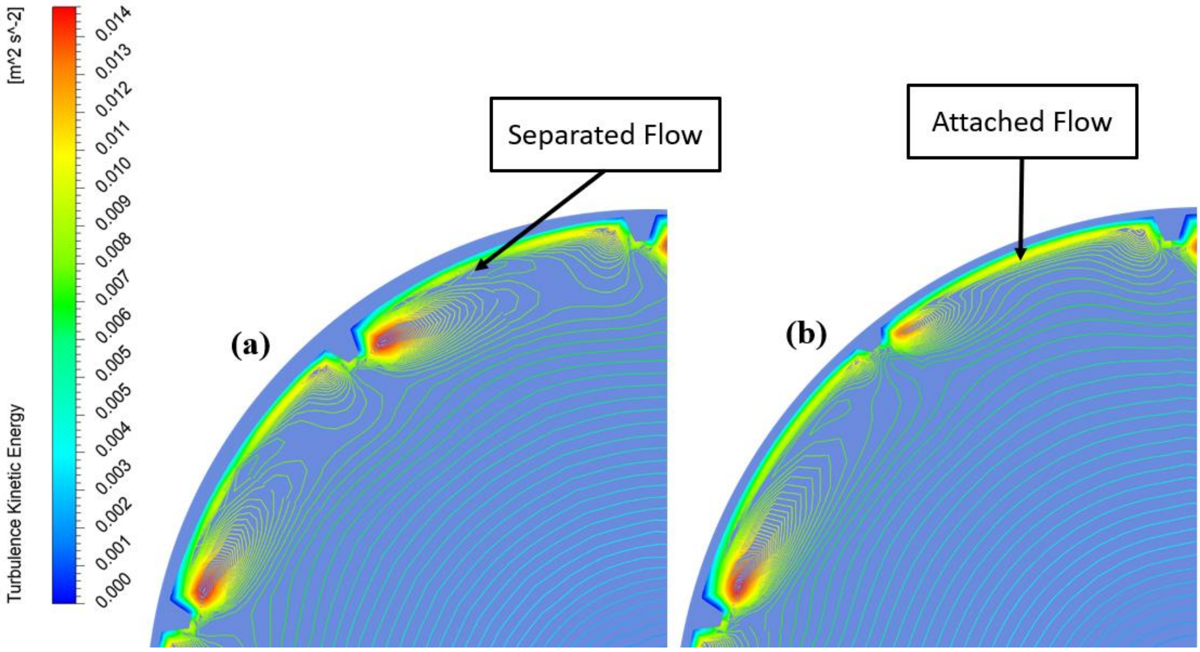

Figure 15: Turbulence kinetic energy contours at Re 54000 for (a) Equal fin height

Pressure drop is higher in 1:1 tube as the Re number is increased as compared to 1:2 tube. Figure 16 shows the local pressure contours at the half length cross-section of both micro-finned tubes. The figure clearly shows slightly higher pressure drop values for equal fin height tube.

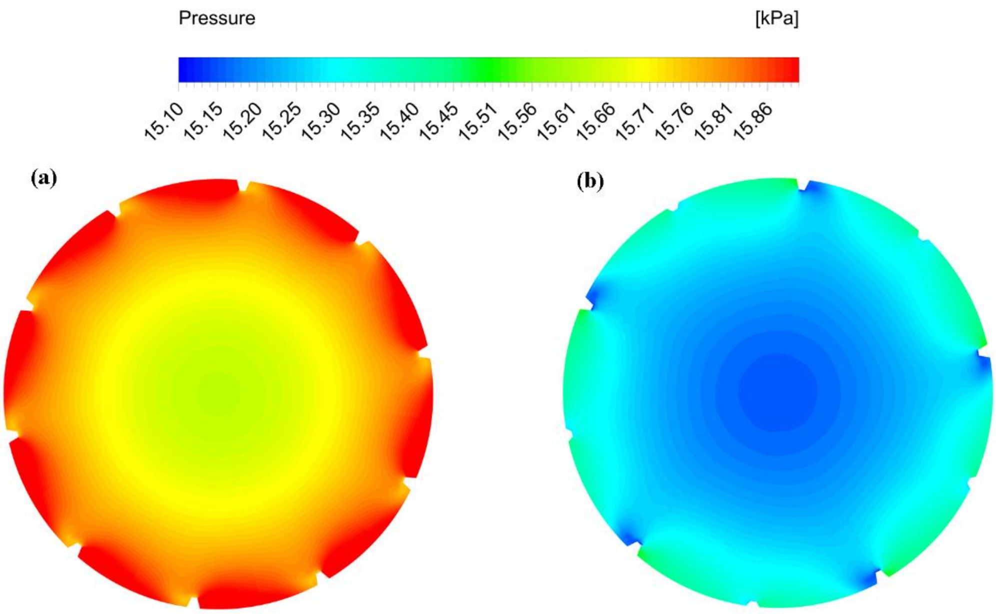

Figure 16: Pressure contours at half length cross-section and Re 54000 for (a) Equal fin height tube (b) Alternating fin height tube

Relative thermal and hydraulic performance of studied tubes is shown in Fig.17. Nusselt number of micro-finned tubes is relatively greater than the smooth tube indicating a higher thermal performance across the whole range of Re. Both the micro-finned tubes showed similar thermal performance. Thermal performance index of micro-finned tubes is greater than smooth tube for lower range of Re and is less than smooth tube for higher Re. This indicates that micro-finned tubes show optimal performance for limited range of Re outside which they have poor performance as compared to smooth tubes. The figure also shows the improved thermal performance of tube with alternating fin height as compared with equal fin height tube. The range of Re in which the finned tubes perform better than smooth tube is also greater for alternating fin height tube.

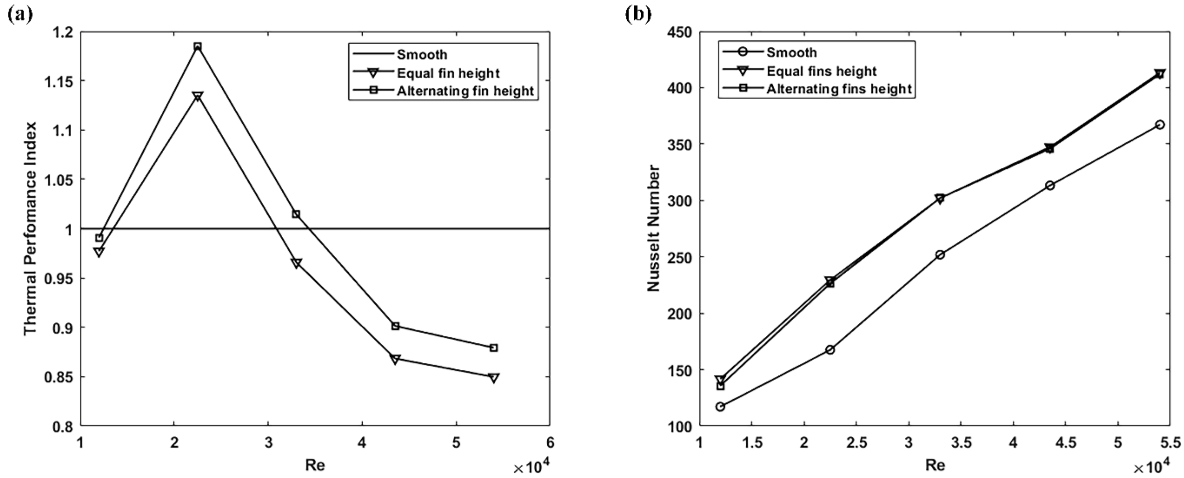

Figure 17: (a) Nusselt number and (b) Thermal performance index of the studied tubes

Normalized friction factor and heat transfer coefficient with respect to smooth for both micro-finned tubes are shown in Fig. 18. The normalization is done to analyse the relative performance of micro-finned tubes with respect to smooth tube and each other.

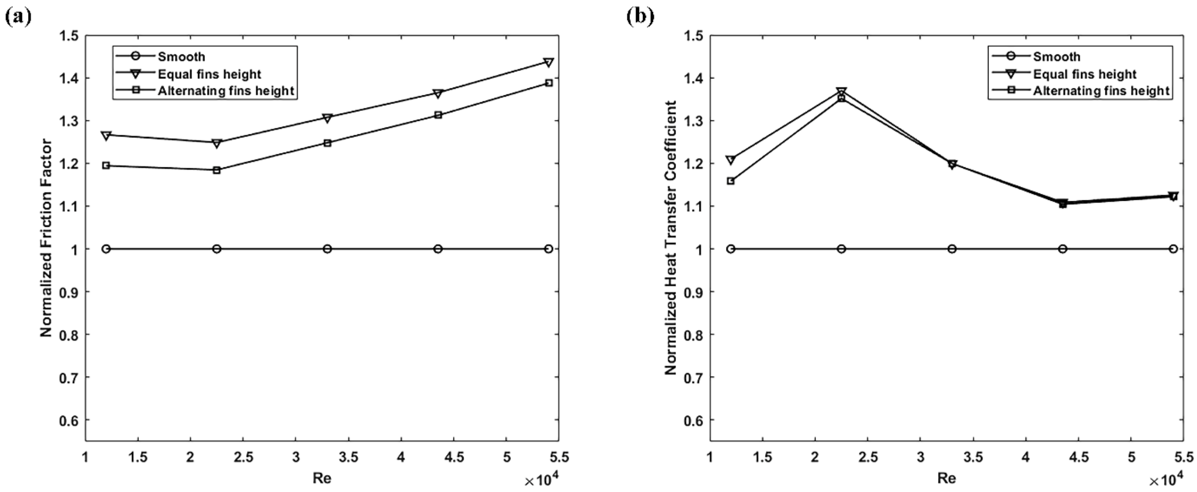

Figure 18: Figure .11 (a) Friction factor and (b) Heat transfer coefficient, normalized with respect to smooth tube.

As compared to smooth tube, both the helically finned tubes show higher heat transfer coefficient and pressure drop. As the Reynolds number increases, the flow is more dominated by pressure drop instead of heat transfer coefficient. Compared to equal fin height tube, alternating fin height tube has lower friction factor across the whole range of Re whereas the heat transfer coefficient is almost the same for the both finned tubes. We can conclude from the above discussion that helically finned tube with alternating fin heights is a better choice for heat transfer augmentation because of the same thermal performance and relatively good hydraulic performance.

CHAPTER 4: CONCLUSIONS AND FUTURE WORK

In this study, numerical simulations of turbulent flow for smooth and internal helically finned tubes with equal and alternating fin height were carried out. Water as working fluid was used with 55°C inlet temperature and walls of the tube were kept at constant temperature of 20°C. A simplified fluid domain was selected instead of complete experimental geometry to demonstrate the proof of concept. The computational solution was validated with the corresponding experimental and numerical work from literature and the results showed relatively good agreement.

It was observed that heat transfer and pressure drop is increased in case of helically finned tubes as compared to smooth tube. An average increase of 32% and 20% in friction factor and heat transfer coefficient respectively is observed in comparison with the smooth tube. The increase in heat transfer and pressure drop occurs due to helically swirling secondary flow near the fins of the micro finned tubes. The flow is dominated by pressure drop at higher Reynolds numbers. Thermal Performance Index of alternating fin height tube is relatively higher than the equal fin height tube. Also, the range of Re in which the Thermal Performance Index is greater than the smooth tube is also broader for alternating fin height tube. The comparative analysis of micro-finned tubes showed that alternating fin height tube has relatively better thermohydraulic performance. An average decrease of 5% in friction factor was achieved at an average cost of <1% loss in heat transfer coefficient for alternating fin height tube as compared with equal fin height tube.

Further investigation may focus on optimized fin-to-fin height ratio. The number of fins and helix angle is kept constant in this study to benchmark the benefits of alternating fin heights. By incorporating all the geometrical parameters of helically finned tube and using a competitive optimization technique, a better passive cooling solution may be achieved.

CHAPTER 5: REFERENCES

[1] S. Kim, M. Kim, Y. G. Park, J. K. Min, and M. Y. Ha, "Numerical investigation of fluid flow and heat transfer characteristics in a helically-finned tube," *Journal of Mechanical Science and Technology,* vol. 31, pp. 3271-3284, 2017.

[2] W.-T. Ji, A. M. Jacobi, Y.-L. He, and W.-Q. Tao, "Summary and evaluation on single-phase heat transfer enhancement techniques of liquid laminar and turbulent pipe flow," *International Journal of Heat and Mass Transfer,* vol. 88, pp. 735-754, 2015.

[3] T. Alam and M.-H. Kim, "A comprehensive review on single phase heat transfer enhancement techniques in heat exchanger applications," *Renewable and Sustainable Energy Reviews,* vol. 81, pp. 813-839, 2018/01/01/ 2018.

[4] S. M. Borhani, M. J. Hosseini, A. A. Ranjbar, and R. Bahrampoury, "Investigation of phase change in a spiral-fin heat exchanger," *Applied Mathematical Modelling,* vol. 67, pp. 297-314, 2019/03/01/ 2019.

[5] L. Duan, X. Ling, and H. Peng, "Flow and heat transfer characteristics of a double-tube structure internal finned tube with blossom shape internal fins," *Applied Thermal Engineering,* vol. 128, pp. 1102-1115, 2018/01/05/ 2018.

[6] S. Huang, H. Zhu, Y. Zheng, Z. Wan, and Y. Tang, "Compound thermal performance of an arc-shaped inner finned tube equipped with Y-branch inserts," *Applied Thermal Engineering,* vol. 152, pp. 475-481, 2019/04/01/ 2019.

[7] S. A. E. Sayed Ahmed, E. Z. Ibrahim, M. M. Ibrahim, M. A. Essa, M. A. Abdelatief, and M. N. El-Sayed, "Heat transfer performance evaluation in circular tubes via internal repeated ribs with entropy and exergy analysis," *Applied Thermal Engineering,* vol. 144, pp. 1056-1070, 2018/11/05/ 2018.

[8] K. Aroonrat and S. Wongwises, "Experimental investigation of condensation heat transfer and pressure drop of R-134a flowing inside dimpled tubes with different dimpled depths," *International Journal of Heat and Mass Transfer,* vol. 128, pp. 783-793, 2019/01/01/ 2019.

[9] J. Chen and W. Li, "Local flow boiling heat transfer characteristics in three-dimensional enhanced tubes," *International Journal of Heat and Mass Transfer,* vol. 121, pp. 1021-1032, 2018/06/01/ 2018.

[10] J. P. Meyer and S. M. Abolarin, "Heat transfer and pressure drop in the transitional flow regime for a smooth circular tube with twisted tape inserts and a square-edged inlet," *International Journal of Heat and Mass Transfer,* vol. 117, pp. 11-29, 2018/02/01/ 2018.

[11] A. Shishkin, F. T. Kanizawa, G. Ribatski, S. Tarasevich, and A. Yakovlev, "Experimental investigation of the heat transfer coefficient during convective boiling of R134a in tubes with twisted tape insert," *International Journal of Refrigeration,* vol. 92, pp. 196-207, 2018/08/01/ 2018.

[12] J. Shi, G. Zheng, and Z. Chen, "Experimental investigation on flow condensation in horizontal tubes filled with annular metal foam," *International Journal of Heat and Mass Transfer,* vol. 116, pp. 920-930, 2018/01/01/ 2018.

[13] X. W. Wang, J. Y. Ho, K. C. Leong, and T. N. Wong, "Condensation heat transfer and pressure drop characteristics of R-134a in horizontal smooth tubes and enhanced tubes fabricated by selective laser melting," *International Journal of Heat and Mass Transfer,* vol. 126, pp. 949-962, 2018/11/01/ 2018.

[14] B. Sajadi, M. Soleimani, M. A. Akhavan-Behabadi, and E. Hadadi, "The effect of twisted tape inserts on heat transfer and pressure drop of R1234yf condensation flow: An experimental study," *International Journal of Heat and Mass Transfer,* vol. 146, p. 118890, 2020/01/01/ 2020.

[15] C. Zhai, M. D. Islam, R. Simmons, and I. Barsoum, "Heat transfer augmentation in a circular tube with delta winglet vortex generator pairs," *International Journal of Thermal Sciences,* vol. 140, pp. 480-490, 2019/06/01/ 2019.

[16] M. Dastmalchi, A. Arefmanesh, and G. Sheikhzadeh, "Numerical investigation of heat transfer and pressure drop of heat transfer oil in smooth and micro-finned tubes," *International Journal of Thermal Sciences,* vol. 121, pp. 294-304, 2017.

[17] S. Eiamsa-ard and K. Wongcharee, "Single-phase heat transfer of CuO/water nanofluids in micro-fin tube equipped with dual twisted-tapes," *International Communications in Heat and Mass Transfer,* vol. 39, pp. 1453-1459, 2012/11/01/ 2012.

[18] A. Celen, A. S. Dalkilic, and S. Wongwises, "Experimental analysis of the single phase pressure drop characteristics of smooth and microfin tubes," *International Communications in Heat and Mass Transfer,* vol. 46, pp. 58-66, 2013.

[19] P. Naphon and P. Sriromruln, "Single-phase heat transfer and pressure drop in the micro-fin tubes with coiled wire insert," *International Communications in Heat and Mass Transfer,* vol. 33, pp. 176-183, 2006/02/01/ 2006.

[20] S. Pirbastami, S. F. Moujaes, and S. G. Mol, "Computational fluid dynamics simulation of heat enhancement in internally helical grooved tubes," *International Communications in Heat and Mass Transfer,* vol. 73, pp. 25-32, 2016.

[21] M. K. Jensen and A. Vlakancic, "Technical Note Experimental investigation of turbulent heat transfer and fluid flow in internally finned tubes," *International Journal of Heat and Mass Transfer,* vol. 42, pp. 1343-1351, 1999.

[22] J. B. Copetti, M. H. Macagnan, D. de Souza, and R. D. C. Oliveski, "Experiments with micro-fin tube in single phase," *International journal of refrigeration,* vol. 27, pp. 876-883, 2004.

[23] D. H. Han and K.-J. Lee, "Single-phase heat transfer and flow characteristics of micro-fin tubes," *Applied Thermal Engineering,* vol. 25, pp. 1657-1669, 2005.

[24] X.-W. Li, J.-A. Meng, and Z.-X. Li, "Experimental study of single-phase pressure drop and heat transfer in a micro-fin tube," *Experimental Thermal and Fluid Science,* vol. 32, pp. 641-648, 2007.

[25] G. J. Zdaniuk, L. M. Chamra, and P. J. Mago, "Experimental determination of heat transfer and friction in helically-finned tubes," *Experimental Thermal and Fluid Science,* vol. 32, pp. 761-775, 2008.

[26] Ö. Ağra, H. Demir, Ş. Ö. Atayılmaz, F. Kantaş, and A. S. Dalkılıç, "Numerical investigation of heat transfer and pressure drop in enhanced tubes," *International Communications in Heat and Mass Transfer*, vol. 38, pp. 1384-1391, 2011.

[27] M. S. Baba, A. V. S. R. Raju, and M. B. Rao, "Heat transfer enhancement and pressure drop of Fe3O4 -water nanofluid in a double tube counter flow heat exchanger with internal longitudinal fins," *Case Studies in Thermal Engineering*, vol. 12, pp. 600-607, 2018/09/01/ 2018.

[28] A. Kumar Solanki and R. Kumar, "Condensation of R-134a inside micro-fin helical coiled tube-in-shell type heat exchanger," *Experimental Thermal and Fluid Science*, vol. 93, pp. 344-355, 2018/05/01/ 2018.

[29] H. Chen, Z. Wan, H. Mo, S. Huang, and Y. Tang, "Experimental studies on the compound thermo-hydraulic characteristics in a 3D inner finned tube with porous copper fiber inserts," *International Communications in Heat and Mass Transfer*, vol. 100, pp. 51-59, 2019/01/01/ 2019.

[30] C.-M. Yang and P. Hrnjak, "Effect of straight micro fins on heat transfer and pressure drop of R410A during evaporation in round tubes," *International Journal of Heat and Mass Transfer*, vol. 117, pp. 924-939, 2018/02/01/ 2018.

[31] ANSYS Fluent 19.0. (2018, 04 jan). *Fluent Theory Guide (19 ed.)*. Available: https://ansyshelp.ansys.com/account/secured?returnurl=/Views/Secured/corp/v190/flu_th/flu_th.html